Investigation of a Side-polished Fiber MZI and Its Sensing Performance

Ping Zhang, Bin Liu, Juan Liu, Cheng-Feng Xie, Sheng-Peng Wan, Xing-Dao He, Xinpu Zhang, Qiang Wu

***Abstract*—A novel all-fiber Mach–Zehnder interferometer (MZI), which consists of lateral core fusion splicing of a short section of side-polished single mode fiber (SMF) between two SMFs was proposed and demonstrated. A simple fiber side-polished platform was built to control the side polished depth through a microscope. The sensitivity of the fiber MZI structure to the surrounding refractive index (RI) can be greatly improved with the increase of the side-polished depth, but has no effect on the temperature sensitivity. The sensor with a polished depth of 44.2 *μm* measured RI sensitivity up to -118.0 *nm*/RIU (RI unit) in the RI range from 1.333 to 1.387, which agrees well with simulation results by using the beam propagation method (BPM). In addition, the fiber MZI structure also can achieve simultaneous measurement of both RI and temperature. These results show its potential for use in-line fiber type sensing application.**

***Index Terms*—Fiber-optic, side-polished, Mach–Zehnder interferometer, refractive index (RI)**

I. Introduction

COMPARED with traditional sensors, optical fiber sensors have advantages such as small size, high sensitivity, anti-electromagnetic interference, and anti-corrosion [1-2]. They have attracted extensive attention and research, and applied in many areas such as biomedicine, construction engineering, navigation, aerospace and chemistry [3]. Various types of fiber optic sensors have been developed, such as fiber Bragg grating [4-6], Fabry-Perot interferometers [7-9], sagnac interferometers [10], surface plasmon resonance [11,12], MZIs [13-15], and so on. Among these optical fiber sensors, optical fiber MZI sensor has unique advantages such as high sensitivity, ease of fabrication, and all-fiber structure [16]. Therefore, optical fiber MZI sensors are used in a variety of applications, not only for temperature measurement [17,18], but also measurements of RI, liquid level, strain, curvature, humidity and other parameters [19-24]. Optical fiber sensors have obvious advantages such as simple fabrication, label-free sensing [25,26]. However, the RI sensitivities of fiber optic MZI sensors are relatively low due to very weak evanescent field of fiber cladding. Furthermore, simultaneous measurement of RI and temperature become an important issue in many areas of study, such as monitoring bacterial growth in biomedical engineering. Due to cross sensitivity, most fiber optic MZI sensors are using to measure a single physical parameter, which cannot satisfy the requirement of simultaneously measurements of multiple parameters. Recently, many fiber-optic processing techniques have been combined with fiber-optic sensor, including tapering [27], etching [28], twisting [29], side-polishing [30] etc. The fiber-optic side polishing technique has been proved to be effectively improving sensing performance [30-31].

In this work, based on the above issues, we propose and investigate a side-polished connection offset (SPCO) fiber MZI structure for simultaneously measurement of both RI and temperature. Theoretical study of the MZI properties and spectral response of RI are provided by using the BPM. Influence of side-polished depth on RI and temperature responses are experimentally investigated. Finally, simultaneous measurement of both RI and temperature are experimentally demonstrated and analyzed.

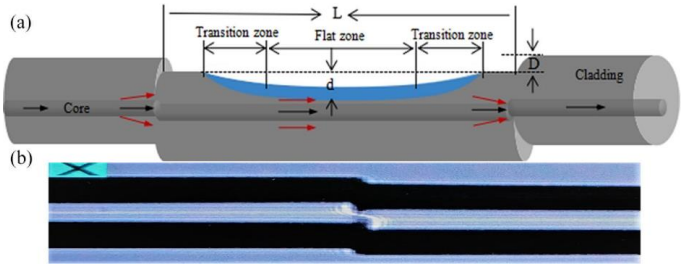

Fig. 1. (a) Structure diagram of side-polished fiber MZI. (b) The photo of offset splicing structure under microscope.

II. Theoretical Analysis and Simulation

A schematic diagram of the proposed SPCO fiber MZI is shown in Fig. 1(a), which is formed by core offset fusion splicing of a short section of SPCO fiber between two SMFs. *L* is the length of the intermediate SMF between two connection offsets, *d* is the polished depth, and *D* is the offset size between two SMFs. Figure 1(b) shows a microphotograph of the fusion splicing offset. As light injected from the broadband source into the input SMF, the first connection offset acts just like a beam splitter, causing the core mode field mismatch of SMF, splitting

This work was jointly supported by National Natural Science Foundations of China (NSFC) (11864025, 61665007); Key project of natural science foundation of Jiangxi (20192ACBL21051, 20192ACB20031). (*Correspondence author*: *Bin Liu and Qiang Wu*)

Ping Zhang, Bin Liu, Juan Liu, Cheng-Feng Xie, Sheng-Peng Wan, and Xing-Dao He were with Key Laboratory of Nondestructive Test (Ministry of Education), Nanchang Hangkong University, Nanchang 330063, China (e-mail: zhangp_5@163.com; liubin@nchu.edu.cn; 65859347@qq.com; xcf@nchu.edu.cn; sp.wan@qq.com; xingdaohe@126.com).

Xinpu Zhang was with Center for Information Photonics and Communications, School of Information Science and Technology, Southwest Jiaotong University, Chengdu, Sichuan 611756, China (e-mail: xpzhang@home.swjtu.edu.cn).

Qiang Wu was with Faculty of Engineering and Environment, Northumbria University, Newcastle Upon Tyne NE1 8ST, UK (e-mail: qiang.wu@northumbria.ac.uk).

the core mode of the input SMF into two bundles for transmission within core and cladding, respectively. The second connection offset acts just as a combiner, where the light of core mode and cladding mode are integrated into core of SMF and generates MZ interference. The intensity of the output of the proposed MZI owing to the interference between the core mode and ith order cladding mode is:

$$I_T = I_1 + I_2 + 2\sqrt{I_1 I_2}\cos(\Delta\varphi) \quad (1)$$

where I_1 and I_2 are the light intensities of the core and i^{th} cladding modes, and $\Delta\varphi$ is the phase difference between them. The wavelength with minimum output light intensity are located at:

$$\lambda_{dip} = \frac{2}{2m+1}(n_{co} - n_{cl})L \quad (2)$$

where n_{co} and n_{cl} are the effective RI of the core and cladding, respectively, and m=0, 1, 2… The evanescent wave of cladding mode was effectively enhanced by side-polishing the fiber, and hence sensitive to the variation of surrounding RI.

The BPM is used to numerically simulate the proposed side-polished MZI fiber sensor. The simulation conditions are based on the mesh size of the 2D model in the *X* and *Z* directions, the grid size is set to 0.1 and 1 *μm*, respectively. The model boundary conditions are based on the perfectly matched layer condition. The core and cladding diameters of the single-mode fiber are 8.2 and 125 *μm*, and the corresponding RIs are 1.4682 and 1.4628, respectively. For polishing depth of 44 *μm and L=3cm*, the simulated transmission spectra of RI response were shown in Fig. 2(a). The interference dip undergoes blue shift as the increase of environmental RI, and the RI sensitivity of linear fit reach -126.5 *nm*/RIU [shown in Fig. 2(b)]. Figure 2(c) and (d) show distributions of the optical field propagating along the MZI and the corresponding normalized optical intensity changes at dip *A* and peak *B*, respectively.

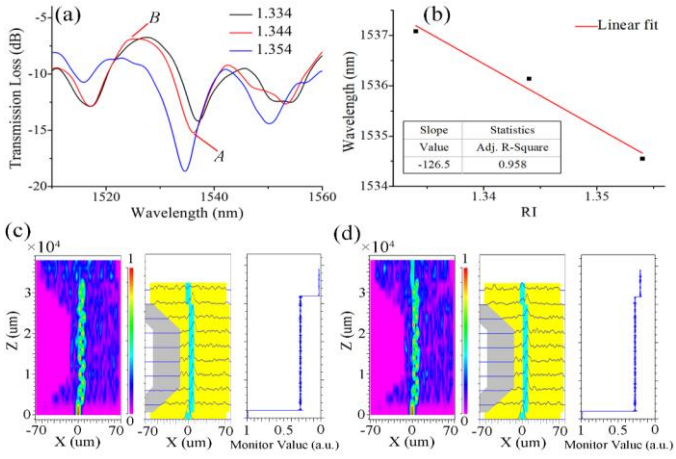

Fig. 2. (a) The simulated spectral response of the side-polished MZI with RI = 1.334, 1.344 and 1.354, respectively; (b) the RI sensing curve; (c) and (d) The distributions of optical field and normalized optical intensity propagating along MZI at dip *A* and peak *B*.

III. Fabrication and Experiments

Firstly, a fiber MZI structure are manufactured by offset fusion splicing technology using traditional fiber fusion splicer (Fujikura 80C). The offset distance of SMF (G652D) is set to 5 *μm* for better interference extinction ratio. To better compare the performance of the fiber MZI sensor after side polishing, the length of the intermediate SMF between two connector offsets set as 3 cm. For fiber side-polishing process, we self-assemble a fiber optic side polishing system [shown in Fig. 3(a)]. A grind wheel with abrasive papers on the fiber side polishing system was used to polish the MZI section, as shown in Fig. 3(a). The prepared MZI fiber structure firstly fixes one end of the fiber to the rotatable fixture of the side polishing system, and then adjusts the position of the fiber MZI structure area to bypass sandpaper-covered grinding wheel, and the other end is also clamped by the rotatable fixture. In order to increase the operability of the fiber and provide a stable and variable tension to the fiber, we designed a device for suspending a weight through a pulley. The weights of different sizes provide the corresponding tension. Finally, after connecting the two ends of the fiber to the light source and the spectrometer through the fiber adapter, respectively, the small motor can be used to control the rotation speed of the grinding wheel to grind the fiber at a constant speed. Replacing sandpaper of different particle sizes can perform different degrees of polishing on the optical fiber. The fiber is roughly polished to a certain depth with sandpaper of 800 mesh. Then we replacing it with 12000 mesh sandpaper for fine polishing, which make the polished surface smooth. The depth of the polished is visually monitored by a microscope connected to a computer, and a high-quality side-polished optical fiber can be produced by the precise operation of the above process. The diameter value of the grinding wheel used for polishing is about 7 *cm*. The length of the flat and transition area are approximately 7.8 *mm* and 9.2 *mm*, respectively. Figures 3(b) shows a microscopic enlarged view of the side polished area. The SEM image of the top polished area in Fig. 3(c) demonstrates that the side-polished surface is very smooth with few scratches. For *L*=3 *cm*, four samples with different polished depths (0, 23.5, 33.8, and 44.2 *μm*) were fabricated for analysis of sensing characteristics.

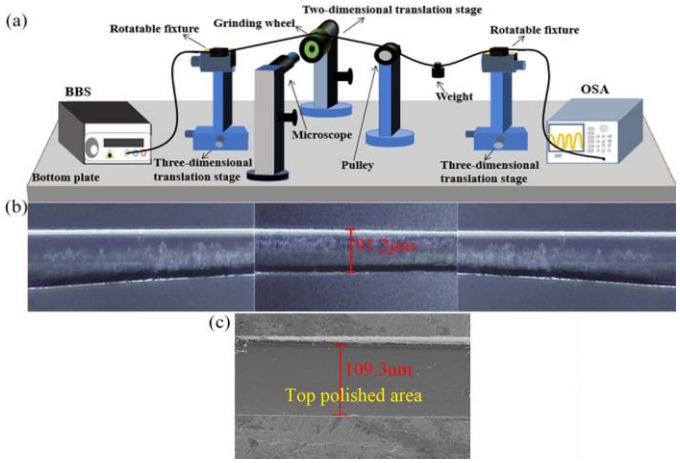

Fig. 3. (a) Fiber side polished system diagram. (b) The photo of side-polished fiber under microscope. (c) The SEM image of the top polished area.

Figure 4 shows the experimental setup for RI and

temperature measurement. The input/output of the SPCO fiber MZI structure are connected to a SC-5-FC broadband light source (BBS) and an optical spectrum analyzer (OSA, YOKOGAWA AQ6370D) for launching/receiving optical signals. In this experiment, in order to minimize the liquid change induced fluctuation to the fiber sensor, we firstly immerse our sensor into a channel filled with water, and then add small amount dimethyl sulfoxide into the channel to allow it diffuse/mix with the water, which will result in RI changes. The wavelength shift will be recorded after it reached steady states and the RI of the mixed water/ dimethyl sulfoxide solution will be calibrated by using an Abbe refractometer. Repeat the process of adding dimethyl sulfoxide into the channel will enable us to measure spectral response of the sensor over different RIs without moving the fiber sensor in/out different RI liquid and hence achieve reliable measurements. In addition, temperature response of the sensor was measured by placing the fiber sensor on a hot plate, where the temperature is calibrated with a thermocouple.

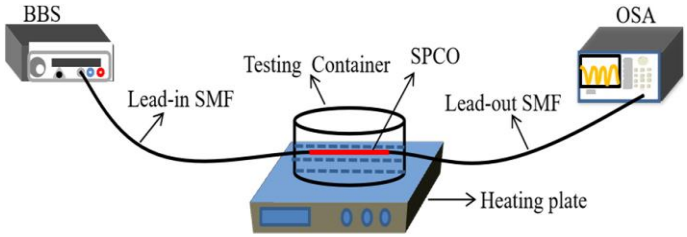

Fig. 4. Structural device for RI and temperature measurement.

IV. Results and Discussion

The experimental results of SPCO fiber MZI structure over different surrounding RI are shown in Fig. 5. Four different SPCO fiber MZI structures with polished depth of 0, 23.5, 33.8, and 44.2 μm were studied and the spectral responses were shown in Figs. 5(a)-(d), respectively. It can be seen that there are a clear blue-shift of the MZI dip for all four fiber MZI structures with the increase of RI. Figures 5(e)-(f) show the dependence of MZI dip wavelength shift on RI for the four fiber MZI structures. There is good linear fitting of RI sensing for all four fiber MZI structures. RI sensitivity of -21.6, -61.3, -92.8 and -118.0 *nm*/RIU correspond to d = 0, 23.5, 33.8 and 44.2 μm, respectively. Moreover, an obvious improvement of RI sensitivities by increasing of polished depth for the SPCO fiber MZI structure. The RI sensitivity (-118.0 *nm*/RIU) of measured MZI dip for d = 44.2 μm agrees very well with the simulated results (-126.5 *nm*/RIU) in Fig. 2.

In addition, the temperature dependence of the SPCO fiber MZI structures with different polished depth is also studied experimentally in Fig. 6. The heating plate, changed the temperature around the SPCO fiber MZI structures, and controlled the temperature from 30 °C to 80 °C, recording once every 10 °C interval, testing the temperature response. The evolutions of transmission spectra versus temperature are shown for the fiber MZI structures with d = 0, 23.5, 33.8, and 44.2 μm, in Figs. 6(a)-(d), respectively. With raising of temperature, the MZI spectra has obvious redshift for all four fiber MZI structures. The linear fit curves and temperature sensitivities were calculated in Figs. 6(e)-(h). There is good linear fitting of temperature sensing for all four fiber MZI structures. The four SPCO fiber MZI structures with d = 0, 23.5, 33.8, and 44.2 μm have the almost the same temperature sensitivities (115.70, 115.54, 119.90 and 113.52 *pm*/°C). The small difference in the magnitude of their temperature sensitivity coefficients may be due to the slight error of length L and the error in the roughness of the polished surface. The results indicate that the temperature response of the proposed sensor is independent on the polished depth.

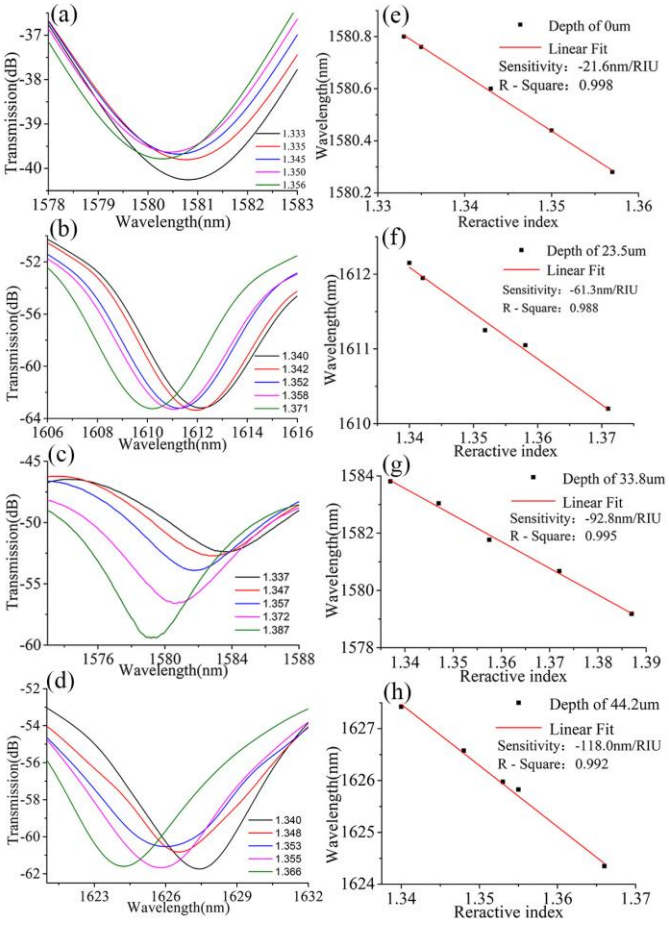

Fig. 5. (a)-(d) transmission spectra response versus RI for the SPCO fiber MZI structure with different polished depths of 0, 23.5, 33.8 and 44.2 μm, respectively; (e)-(h) Dip wavelength shift as a function of RI.

Finally, due to breaking circular-symmetrical of optical fiber cladding cross-section by side-polishing process, when light passes through the side-polishing fiber MZI structure, two orthogonal polarization cladding modes have different RI responses [27]. The cladding mode whose field distribution parallel to the side-polished direction has a larger evanescent field than that perpendicular to the side-polished direction. So, when they interfere with the core mode of SMF, different interference dips will have different response over the surrounding RI variations. However, the temperature response results of the SPCO fiber MZI structure revealed that side-polish depth has no influence on the temperature sensitivity. Based on the feature of SPCO fiber MZI structure,

the simultaneous measurement of both surrounding RI and temperature are investigated as shown in Fig. 7. Figures 7(a) and (b) show the transmission spectra response of the two different interference dips with the changes of RI and temperature. Figures 7(c) and (d) illustrate wavelength shifts of dip1 and dip2 as a function of RI and temperature, respectively. The RI sensitivities of dip1 and dip2 are -115.6 *nm*/RIU and -5.1 *nm*/RIU, respectively. The temperature sensitivities of dip1 and dip2 are 114.77 *pm*/°C and 119.87 *pm*/°C, respectively.

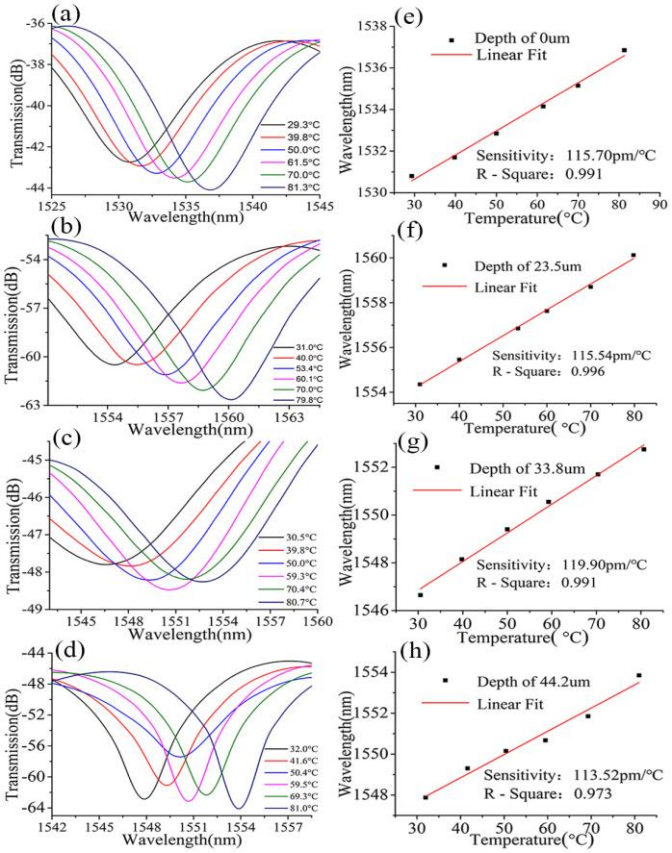

Fig. 6 (a)-(d) transmission spectra response versus temperature for the SPCO fiber MZI structure with different polished depths of 0, 23.5, 33.8 and 44.2 μm, respectively; (e)-(h) Dip wavelength shift as a function of temperature.

According to the experimental results, dip1 and the dip2 have different RI and temperature sensitivities, which can achieve dual parameter measurement through the following coefficient matrix:

$$\begin{bmatrix} \Delta\lambda_1 \\ \Delta\lambda_2 \end{bmatrix} = \begin{bmatrix} K_{n1} & K_{t1} \\ K_{n2} & K_{t2} \end{bmatrix} \begin{bmatrix} \Delta n \\ \Delta T \end{bmatrix} \tag{3}$$

where $\Delta\lambda_1$ and $\Delta\lambda_2$ are the wavelength drifts of dip1 and dip2, respectively. K_{n1}, K_{n2}, and K_{t1}, K_{t2} are RI and temperature response sensitivities of dip1 and dip2, respectively. Δn and ΔT are the amount of changes in RI and temperature of dip1 and dip2, respectively. All these parameters can be calibrated/measured using our proposed sensor. The matrix can thus be inversely transformed to obtain the measurement matrix:

$$\begin{bmatrix} \Delta n \\ \Delta T \end{bmatrix} = \frac{1}{D} \begin{bmatrix} K_{t2} & -K_{t1} \\ -K_{n2} & K_{n1} \end{bmatrix} \begin{bmatrix} \Delta\lambda_1 \\ \Delta\lambda_2 \end{bmatrix} \tag{4}$$

where $D = K_{n1}K_{t2} - K_{n2}K_{t1}$, substituting the RI and temperature sensitivity coefficients of dip1 and dip2 measured in the experiment. The relationship between the amount of wavelength drift and the two parameters of RI and temperature can be obtained that:

$$\begin{bmatrix} \Delta n \\ \Delta T \end{bmatrix} = \frac{1}{-13.271645} \begin{bmatrix} 0.11987 & -0.11477 \\ 5.1 & -115.6 \end{bmatrix} \begin{bmatrix} \Delta\lambda_1 \\ \Delta\lambda_2 \end{bmatrix} \tag{5}$$

Therefore, when RI and temperature of the external environment change simultaneously, the amount of change in temperature and RI can be obtained by measuring the wavelength shift of dip1 and dip2, and thus simultaneous measurement of refractive index and temperature can be realized.

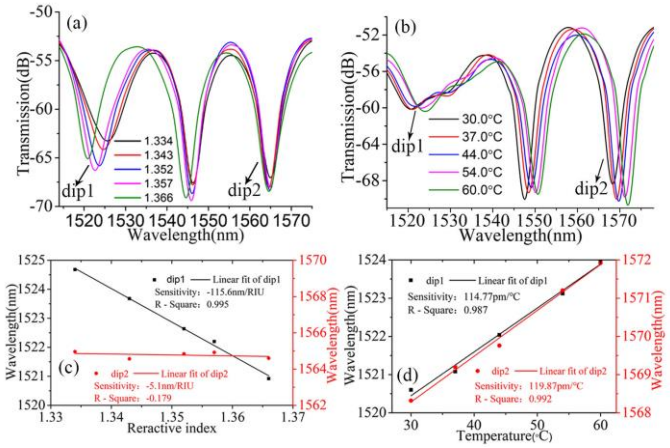

Fig. 7. Transmission spectra of dip1 and dip2: (a) versus RI; (b) versus temperature. Linear fit diagram of dip1 and dip2 wavelength shift: (a) versus RI; (b) versus temperature.

V. Conclusion

In conclusion, a novel SPCO fiber MZI is reported for the first time, which fabricated from a core offset fusion splicing SMF by employing side polishing technique. Simulation results demonstrate a good RI sensing for the fiber MZI structures. Four SPCO fiber MZI samples with different side-polished depth values (d = 0, 23.5, 33.8, and 44.2 μm) were fabricated, and their RI and temperature response characteristics were tested in detail. The experimental results demonstrate that a greatly improve of RI sensitivity as increasing of side-polished depth. The measured average RI sensitivity is as high as -118.0 *nm*/RIU in the RI range from 1.334 to 1.39 with d = 44.2 μm. But the side-polished process hardly affects temperature sensitivity for the fiber MZI structure. In addition, for breaking circular-symmetrical of optical fiber cross-section by side-polishing process, simultaneous measurement of both RI and temperature also can achieved for the fiber MZI structure. The sensor has the advantages of high sensitivity, simple structure and low cost, and can be applied to the fields of chemical and biological sensing.

REFERENCES

[1] D. D. Pang and Q. M. Sui, "A relocatable resonant FBG-acoustic emission sensor with strain-insensitive structure," *Optoelectronics Letters*, vol. 10, no. 2, pp. 96–99, Mar. 2014.

[2] H. Y. Fu, S.W. Zhang, H. Chen, and J. Weng, "Graphene Enhances the Sensitivity of Fiber-Optic Surface Plasmon Resonance Biosensor," *IEEE Sensors J*., vol. 15, no. 10, pp. 5478–5482, Jun. 2015.

[3] C. Y. He, J. B. Fang, Y. N. Zhang, Y. Yang, J. H. Yu, J. Zhang, H.Y. Guan, W. T. Qiu, P. J. Wu, J. L. Dong, H. H. Lu, J. Y. Tang, W. G. Zhu, N. Arsad, Y. Xiao, and Z. Chen, "High performance all-fiber temperature sensor based on coreless side-polished fiber wrapped with polydimethylsiloxane," *Opt. Exp*., vol. 26, no. 8, pp. 9686–9699, Apr. 2018.

[4] Y. N. Zhu, P. Shum, H. J. Chong, M. Rao, and C. Lu, "Strong resonance and a highly compact long period grating in a large-mode-area photonic crystal fiber," *Opt. Exp*., vol. 11, no. 16, pp. 1900–1905, Aug. 2003.

[5] S. J. Qiu, Y.Chen, J. L. Kou, F. Xu, and Y. Q. Lu, "Miniature tapered photonic crystal fiber interferometer with enhanced sensitivity by acid microdroplets etching," *Appl. Opt*., vol. 50, no. 22, pp. 4328–4332, Aug. 2011.

[6] Q. Wang, C. Du, J. Zhang, R. Lv, and Y. Zhao, "Sensitivity-enhanced temperature sensor based on PDMS-coated long period fiber grating," *Opt. Commun*., vol. 377, pp. 89–93, Oct. 2016.

[7] W. Xu, W. B. Huang, X. G. Huang, and C. Y. Yu, "A simple fiber-optic humidity sensor based on extrinsic Fabry-Perot cavity constructed by cellulose acetate butyrate film," *Opt. Fiber Technol*., vol. 19, no. 6, pp. 583–586, Dec. 2013.

[8] W. J. Xie, M. H. Yang, Y. Cheng, D. W. Li, Y. Zhang, and Z. Zhuang, "Optical fiber relative-humidity sensor with evaporated dielectric coatings on fiber end-face," *Opt. Fiber Technol*., vol. 20, no. 4, pp. 314–319, Aug. 2014.

[9] H. Sun, X. L. Zhang, L. T. Yuan, L. B. Liu, and M. L. Hu, "An optical fiber Fabry-Perot interferometer sensor for simultaneous measurement of relative humidity and temperature," *IEEE Sensors J*., vol. 15, no. 5, pp. 2891–2897, May 2015.

[10] Y. Zhao, X. Liu, R. Q. Lv, and Q. Wang, "Simultaneous measurement of RI and temperature based on the combination of Sagnac loop mirror and balloon-like interferometer," *Sens. Actuators B, Chem*., vol. 243, pp. 800–805, May 2017.

[11] Singh, Sarika, S. K. Mishra, and B. D. Gupta, "Sensitivity enhancement of a surface plasmon resonance based fibre optic refractive index sensor utilizing an additional layer of oxides," *Sens. Actuators A, Phys*., vol. 193, pp. 136–140, Apr. 2013.

[12] Z. W. Ding, T. T. Lang, Y. Wang, and C. L. Zhao, "Surface Plasmon Resonance Refractive Index Sensor Based on Tapered Coreless Optical Fiber Structure," *J. Lightwave Technol*., vol., 35, no. 21, pp. 4734–4739, Nov. 2017.

[13] F. D. Yu, P. Xue, X. W. Zhao, and J. Zheng, "Simultaneous Measurement of Refractive Index and Temperature Based on a Peanut-Shape Structure In-Line Fiber Mach-Zehnder Interferometer," *IEEE Sensors J*., vol. 19, no. 3, pp. 950–955, Feb. 2019.

[14] K. Ni, C. C. Chan, L. H. Chen, X. Y. Dong, R. Huang, and Q. F. Ma, "A chitosan-coated humidity sensor based on Mach-Zehnder interferometer with waist-enlarged fusion bitapers," *Opt. Fiber Technol*., vol. 33, pp. 56–59, Jan. 2017.

[15] M. Sun, B. Xu, X. Y. Dong, and Y. Li, "Optical fiber strain and temperature sensor based on an in-line Mach–Zehnder interferometer using thin-core fiber," *Opt. Commun*., vol. 285, no. 18, pp. 3721–3725, Aug. 2012.

[16] Y. Gong, T. Zhao, Y. J. Rao, and Y. Wu, "All-fiber curvature sensor based on multimode interference," *IEEE Photon. Technol. Lett*., vol. 23, no. 11, pp. 679–681, Jun. 2011.

[17] D. P. Zhou, L. Wei, W. K. Liu, and W. Y. Lit. John, "Simultaneous Strain and Temperature Measurement With Fiber Bragg Grating and Multimode Fibers Using an Intensity-Based Interrogation Method," *IEEE Photon. Technol. Lett*., vol. 21, no. 7, pp. 468–470, Apr. 2009.

[18] Y. C. Liao, B. Liu, J. Liu, S. P. Wan, X. D. He, J. H. Yuan, X. Y. Fan, and Q. Wu, "High Temperature (Up to 950 °C) Sensor Based on Micro Taper In-Line Fiber Mach–Zehnder Interferometer," *Appl. Sci*., vol. 9, no. 12, pp. 2394, Jun. 2019.

[19] J. Chen, J. Zhou, Q. Zhang, H. Zhang and M. Chen, "All-fiber modal interferometer based on a joint-taper-joint fiber structure for refractive index sensing with high sensitivity ," *IEEE Sensors J*., vol. 13, no. 7, pp. 2780–2785, Jul. 2013.

[20] J. M. Hsu, C. L. Lee, H. P. Chang, W. C. Shih, and C. M. Li, "Highly sensitive tapered fiber mach–zehnder interferometer for liquid level sensing," *IEEE Photon. Technol. Lett*., vol. 25, no. 14, pp. 1354–1357, Jul. 2013.

[21] Q. Wu, A. Muhamad Hatta, Y. Semenova, and G. Farrell, "Use of a single-multiple-single-mode fiber filter for interrogating fiber Bragg grating strain sensors with dynamic temperature compensation," Appl. Opt., vol. 48, no. 29, pp. 5451–5458, Oct. 2009.

[22] H. P. Gong, H. F. Song, X. R. Li, J. F. Wang, and X. Y. Dong, "An optical fiber curvature sensor based on photonic crystal fiber modal interferometer," *Sens. Actuators A, Phys*., vol. 195, no. 6, pp. 139–141, Jun. 2013.

[23] X. F. Wang, K. Tian, L. B. Yuan, E. Lewis, G. Farrell, and P. F Wang, "A High-Temperature Humidity Sensor Based on a Singlemode-Side Polished Multimode-Singlemode Fiber Structure," *J. Lightwave Technol*., vol. 36, no.13, pp. 2730–2736, Jul. 2018.

[24] Y. Liu, A. Zhou, and L. B. Yuan, "Gelatin-Coated Michelson Interferometric Humidity Sensor Based on a Multicore Fiber With Helical Structure," *J. Lightwave Technol*., vol. 37, pp. 2452–2457, May 2019.

[25] S. J. Duan, X. Y. Bai, X. Y. Kang, H. Du, W. L. Liu, T. Geng, C. G. Tong, C. T. Sun, X. R. Jin, C. L. Lu, Y. X. Li, W. M. Sun, and L. B. Yuan, "High Sensitive Torsion Sensor Based on Cascaded Pre-Twisted Taper and Multi-Mode Fiber Sheets," *IEEE Photon. Technol. Lett.*, vol. 31, no. 19, pp. 1588–1591, Oct. 2019.

[26] Z. Li, C. Liao, D. Chen, J. Song, W. Jin, G. Peng, F. Zhu, Y. Wang, J. He, and Y. Wang, "Label-free detection of bovine serum albumin based on an in-fiber Mach-Zehnder interferometric biosensor," *Opt. Exp*., vol. 23, no. 5, pp. 6673–6678, Jul. 2017.

[27] L. Sun, Z. Yuan, T. Huang, Z. Sun, W. Lin, Y. Huang, P. Xiao, M. Yang, J. Li, and B. Guan, "Ultrasensitive sensing in air based on Sagnac interferometer working at group birefringence turning point," *Opt. Exp*., vol. 27, no. 21, pp. 29501–29509, Oct. 2019.

[28] Q. Wu, Y. Semenova, P. Wang, and G. Farrell, "High sensitivity SMS fiber structure based refractometer-analysis and experiment," *Opt. Exp*., vol. 19, no. 9, pp. 7937–7944, Apr. 2011.

[29] K. Tian, G. Farrell, X. Wang, W. Yang, Y. Xin, H. Liang, E. Lewis, P. Wang, "Strain sensor based on gourd-shaped single-mode-multimode-single-mode hybrid optical fiber structure," *Opt. Exp*., vol. 25, no. 16, pp. 18885–18896, Aug. 2017.

[30] X. Wang, G. Farrell, E. Lewis, K. Tian, L. Yuan, and P. Wang, "A humidity sensor based on a singlemode-side polished multimode-singlemode (SSPMS) optical fiber structure coated with gelatin," *J. Lightwave Technol*., vol. 35, no. 18, pp. 4087–4094, Sep. 2017.

[31] Y Dong, S. Y. Xiao, B. L. Wu, H. Xiao, S. S. Jian, "Refractive Index and Temperature Sensor Based on D-Shaped Fiber Combined with A Fiber Bragg Grating," *IEEE Sensors J*., vol. 19, no. 4, pp. 1362–1367, Feb. 2019.

Ping Zhang received the B.S. degree from Hefei Normal University in 2018. He is currently pursuing the M.S. degree in optical engineering with Nanchang Hangkong University. His current research interests include optical fiber sensing theory and technology.

Bin Liu was born in Nanchang, Jiangxi Province, China, in 1983. He received the B.S. degree from School of physics Sun Yat-sen University in 2004; M.S. and Ph.D. degrees from School of physics Sun Yat-sen University in 2010. He is currently an associate Professor with Jiangxi Engineering Laboratory for Optoelectronics Testing Technology, Nanchang Hangkong University, Nanchang, China. His work interests include optical fiber sensing theory and technology, Design of micro/nano photonic devices, and Optical nonlinear dynamics.

Juan Liu received the Ph.D. degree from Beijing Normal University in 2010. From 2010 to 2019, She is a teacher with Jiangxi Engineering Laboratory for Optoelectronics Testing Technology, Nanchang Hangkong University, Nanchang,

China. Her work interests include optical sensing theory and technology.

Cheng-Feng Xie received the Ph.D. degree from North University of China. He is a teacher with Jiangxi Engineering Laboratory for Optoelectronics Testing Technology, Nanchang Hangkong University, Nanchang, China. His research interests are mainly focused on optical fiber sensing technology and their applications.

Sheng-Peng Wan was born in Nanchang, China, in 1971. He received the Ph.D. degree in optics from University of Electronic Science and Technology of China, Chengdu, China, in 2002. He was a Postdoc with the Center of Optical and Electromagnetic Research, Zhejiang University, during 2003–2005. He is currently a Professor with Jiangxi Engineering Laboratory for Optoelectronics Testing Technology, Nanchang Hangkong University, Nanchang, China. His current research interests include optical fiber sensors and OCDMA.

Xing-Dao He was born in Jingan, Jiangxi Province, China, in 1963. He received the Ph.D. degree in optics from Beijing Normal University, Beijing, China, in 2005. He is currently a Director and a Professor of Jiangxi Engineering Laboratory for Optoelectronics Testing Technology, Nanchang Hangkong University, Nanchang, China. His current research interests include Brillouin scattering and spectroscopic techniques.

Xinpu Zhang received the Ph.D. degree in optical engineering degrees in Dalian University of Technology in 2016. He is currently a teacher in School of information science and technology, southwest jiaotong university. His research interests are mainly focused on Optical fiber sensing technology and its application, micro and nano optoelectronic devices, new optoelectronic materials, preparation and application of optical fiber lasers and optical fiber gratings.

Qiang Wu received the B.S. degree in physics from Beijing Normal University, Beijing, China, and the Ph.D. degree from Beijing University of Posts and Telecommunications, Beijing, China, in 1996 and 2004, respectively. He was a Senior Research Associate with the Optoelectronics Research Centre, City University of Hong Kong, a Research Associate with the Applied Optics and Photonics Group, Heriot-Watt University, and a Stokes Lecturer and Fiosraigh Principal Investigator with the Photonics Research Centre, Dublin Institute of Technology. He is currently an Associate Professor with the Department of Mathematics, Physics, and Electrical Engineering, Northumbria University, Newcastle Upon Tyne, U.K. His current research interests include optical fiber interferometers for novel fiber optical couplers and sensors, nanofiber, microsphere sensors for biochemical sensing, design and fabrication of fiber grating devices, and their applications for sensing, nonlinear fiber optics and surface plasmon resonant. He has more than 200 publications in the area of photonics. He is a Committee Member of Holography and Optical Information Processing committee, The Chinese Optical Society, a member of Editorial Board of Scientific Reports and an Associate Editor of the IEEE SENSORS JOURNAL.